Shear Deformation Theory for Compressive Delamination Buckling and Growth

Hsin-Piao Chen*
California State University, Long Beach, Long Beach, California 90840

The elastic buckling and postbuckling analyses of an axially loaded beamplate with an across-the-width delamination symmetrically located at an arbitrary depth are studied. A variational-principle-consistent shear deformation theory coupled with a Griffith-type fracture criterion is developed to formulate the problem. The results for various length ratios and thickness ratios of delamination vs plate are calculated and compared with those without the transverse shear effect. It is indicated that the effect of shear deformation always lowers the critical buckling load and the ultimate load of the delaminated plate. The extent of this reduction depends on the ratio of inplane axial Young's modulus to transverse shear modulus and the length ratio and thickness ratio of delamination to plate. The energy release rate at the crack tip can be expressed in an analytic form. The results of the analysis show that, for the same applied load, the energy release rate is larger with transverse shear effect included. Therefore, the initiation of delamination growth will occur at a lower applied load than that evaluated with the classical lamination theory.

Introduction

DELAMINATION is one of the most common failure modes of composite materials. It may occur as a consequence of the imperfections in the production process or the effects of external factors during the operational life of the composite laminates, such as the impact by foreign objects. The presence of delamination in a laminated composite material may reduce the overall stiffness and cause material unbalance in an otherwise symmetric laminate. This, in turn, may lower the buckling load of the laminate and lead to global structural failure at loads below the design level.

The initiation, development, and termination of delamination buckling and growth in a compressed laminate depend strongly on various geometrical parameters, material properties, and loading conditions. Investigation of the effects of these parameters, and the ways in which they combine to produce qualitatively different types of buckling and growth behavior, has been an active research topic recently.[1-10] Most studies on the subject of delamination buckling and growth were based on the static postbuckling solutions of homogeneous or laminated plates. The energy release rate is used in the analysis and the Griffith-type fracture criterion with a constant specific fracture energy is assumed in these studies. Different methods were used to obtain the energy release rate. These include the differentiation of the total strain energy with respect to the delamination length by Chai et al.[1] and Chow and Ngan,[11] a finite element method to compute the crack closure integral by Whitcomb,[2] and the path independent J integral by Yin and Wang.[12] Dynamic analysis of the growth for a thin, homogeneous, strip delamination in a thick, axially loaded base plate was studied[13-15] recently. A variational-principle-consistent approach was chosen by Chen and Ngo[15] to derive the governing equations of the dynamic delamination postbuckling and growth behavior for a near surface strip delamination. The local growth condition at the delamination front was obtained as one of the natural boundary conditions from the variational energy principle.

For the previous work just mentioned, the effects of transverse shear on delamination buckling, postbuckling, and growth are seldom considered. However, the effects of transverse shearing stresses are important for composite laminates due to the fact that, in composite fiber reinforced materials, the interlaminar shear moduli are usually much smaller than the inplane Young's moduli. For laminated plates subjected to bending loads, the solutions based on classical lamination theory showed significant departures from the exact elasticity solutions for cases with low ratios of inplane dimensions to thickness. As a result, it is necessary to use a shear deformation theory when problems of delamination buckling, postbuckling, and growth are considered for moderately thick plates. Recently, Kardomateas and Schmueser[16] made some studies about the effects of transverse shearing forces on buckling and postbuckling of delaminated composites under compressive loads. Their studies were based on the classical engineering solutions (Euler loads, etc.) of beam-columns with transverse shear correction terms added to account for the shear effects. In the present work, a variational energy principle approach is used to formulate the problem instead. It is believed that this approach is more general and is more systematic in formulation.

A specially orthotropic rectangular plate axially loaded (either loading control or displacement control) between two clamped edges is considered. It is assumed that an across-the-width delamination at an arbitrary depth from the top surface is located symmetrically with respect to the two clamped edges and remains so in the course of delamination growth. The problem is formulated by a variational energy principle. The transverse shear effect is included and a moving boundary condition at the delamination front based on a Griffith-type fracture criterion is considered. From the variational energy principle, the governing equations of static delamination buckling, postbuckling, and growth are derived, which included the following: 1) six equations of equilibrium for the deflections and rotations in three divided segments; 2) four geometric boundary conditions for the deflections and rotations at the edge of plate and the midpoint of the plate; 3) four continuity conditions for the deflections and rotations at the intersections of base plate, lower segment, and upper segment; 4) a compatibility condition for the axial displacement; 5) four natural (or force) boundary conditions including the zero slopes of the deflections at the midpoint of the plate for both the upper and lower segments, moment balance condition, and shear force balance condition at the delamination front; 6) an equilibrium equation of axial forces; 7) an expression for

Received March 16, 1990; presented as Paper 90-1022 at the AIAA/ASME/ASCE/AHS/ASC 31st Structures, Structural Dynamics, and Materials Conference, Long Beach, CA, April 2-4, 1990; revision received May 28, 1990; accepted for publication May 29, 1990.

*Associate Professor, Department of Aerospace Engineering. Member AIAA.

total axial shortening (this equation is used for the displacement-controlled problem); and 8) a local delamination growth condition at the crack tip. One of the advantages of the variational energy principle approach is that the local growth condition at the crack tip and the energy release rate can be derived as the natural outcome from the formulation. The J integral[12] is not necessarily used to determine the energy release rate. General expressions of deflections and rotations of the postbuckling solution can be obtained. A nonlinear algebraic equation is derived to calculate the critical buckling load of the delaminated plate. For the loading-controlled case, two nonlinear algebraic equations are obtained to determine the amplitude of deflections and compressive force in the delaminated segments. For the displacement-controlled case, one more nonlinear algebraic equation for axial shortening of the laminate is needed to solve the problem. The energy release rate at the crack tip can be expressed analytically in terms of the axial forces, the bending moments, the transverse shear forces, and the slopes of the deflections of the three segments at the delamination front in the postbuckling configuration.

Formulation

The delamination buckling, postbuckling, and growth in a specially orthotropic rectangular plate axially loaded (either loading control or displacement control) between two clamped edges are considered. The geometry of the model is shown in Fig. 1. Because of the symmetry of the model, only half of the plate is considered and is divided into three segments referred separately as base plate (sublaminate 1), lower sublaminate (sublaminate 2), and upper sublaminate (sublaminate 3). Let $2a$ and $2l$ be the lengths of the delaminated segment and the whole plate, respectively, and h and H be the thicknesses of the upper sublaminate and the base plate, respectively. The transverse deflections w_i and rotations ψ_i $(i = 1,2,3)$ must satisfy the following geometric boundary conditions:

$$w_1(l) = 0, \qquad \psi_1(l) = 0 \tag{1}$$

$$\psi_2(0) = 0, \qquad \psi_3(0) = 0 \tag{2}$$

The continuity conditions for the deflections and rotations at the delamination front are

$$w_1(a) = w_2(a) = w_3(a) \tag{3}$$

$$\psi_1(a) = \psi_2(a) = \psi_3(a) \tag{4}$$

Furthermore, the axial force balance condition and the compatibility condition for the axial displacement require that

$$P_1 = P_2 + P_3 \tag{5}$$

$$(1-\nu_{13}\nu_{31})\frac{P_3 a}{Eh} + \frac{1}{2}\int_o^a (w_{3,x})^2 dx = (1-\nu_{13}\nu_{31})\frac{P_2 a}{E(H-h)} + \frac{1}{2}\int_o^a (w_{2,x})^2 dx - \frac{\psi_3(a)H}{2} \tag{6}$$

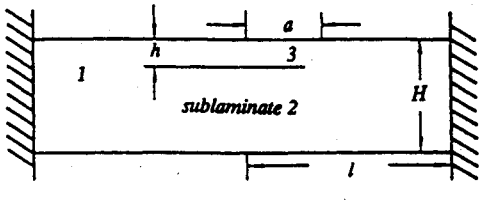

Fig. 1 Geometry of delamination buckling.

where E, ν_{13}, and ν_{31} are the inplane Young's modulus in the axial direction, major and minor Poisson's ratios in xz plane, respectively. The P_i $(i = 1,2,3)$ are the compressive forces of the corresponding sublaminates. For displacement controlled problems, the axial shortening Δ of the delaminated plate must satisfy the following relation

$$\Delta = \frac{(1-\nu_{13}\nu_{31})P_1}{EH}(l-a) + \frac{1}{2}\int_a^l w_{l,x}^2 dx + \frac{(1-\nu_{13}\nu_{31})P_3}{Eh}a + \frac{1}{2}\int_o^a w_{3,x}^2 dx + \frac{H-h}{2}\psi_3(a) \tag{7}$$

The total potential energy Π for half of the plate can be expressed as

$$\Pi = (U_b + U_m + U_s) + V + E_f \tag{8}$$

where U_b, U_m, U_s are strain energies of bending, membrane, and shear, respectively; V is the external potential energy of the applied load P_1; and E_f is the fracture energy of the material. The definitions of these terms are as follows:

$$U_b = \frac{1}{2}\int_a^l D_1\psi_{1,x}^2 dx + \frac{1}{2}\int_o^a D_2\psi_{2,x}^2 dx + \frac{1}{2}\int_o^a D_3\psi_{3,x}^2 dx \tag{9}$$

$$U_m = \frac{1-\nu_{13}\nu_{31}}{2E}\left\{\frac{P_2^1(l-a)}{H} + \frac{P_2^2 a}{H-h} + \frac{P_3^2 a}{h}\right\} \tag{10}$$

$$U_s = \frac{1}{2}\int_a^l kG(\psi_1 + w_{1,x})^2 H\, dx + \frac{1}{2}\int_o^a kG(\psi_2 + w_{2,x})^2 \times (H-h)dx + \frac{1}{2}\int_o^a kG(\psi_3 + w_{3,x})^2 h\, dx \tag{11}$$

$$V = -P_1\Delta \tag{12}$$

$$E_f = \Gamma^*(a-a_o) \tag{13}$$

where $D_1[= EH^3/12(1-\nu_{13}\nu_{31})]$, D_2, D_3 are the bending stiffnesses for the corresponding sublaminates, respectively, G is the transverse shear modulus, k the shear correction factor, Γ^* the specific fracture energy of the material that is defined to be the energy required to create a unit of new delamination surface, and a_o the initial length of the delaminated layer. The transverse shear effect is included in the formulation. The equations of equilibrium, the natural boundary conditions, the energy release rate, and the local growth condition at the delamination front are then derived from the variational energy principle. One advantage of the present approach is that the local growth condition at the crack tip and the energy release rate can be obtained as the natural outcome. The variational principle requires

$$\delta\Pi = \delta U_b + \delta U_m + \delta U_s + \delta V + \delta E_f = 0 \tag{14}$$

After a series of routine but tedious variational operations on deflections w_i, rotations ψ_i, $(i = 1,2,3)$, and delamination length a, the equilibrium equations for each sublaminate are derived as the following:

$$D_i\psi_{i,xx} - kGh_i(\psi_i + w_{i,x}) = 0, \qquad i = 1, 2, 3 \tag{15}$$

$$kGh_i(\psi_{i,x} + w_{i,xx}) - P_i w_{i,xx} = 0, \qquad i = 1, 2, 3 \tag{16}$$

where

$$h_1 = H, \qquad h_2 = H - h, \qquad h_3 = h \tag{17}$$

Two natural boundary conditions at the midpoint of the plate are obtained as

$$w_{2,x}(0) = 0, \qquad w_{3,x}(0) = 0 \tag{18}$$

The other two natural boundary conditions at the delamination front can be written as

$$(D_1\psi_{1,x} - D_2\psi_{2,x} - D_3\psi_{3,x}) + \frac{1}{2}[(H-h)P_3 - hP_2] = 0 \quad \text{at} \quad x = a \tag{19}$$

$$[kGH(\psi_1 + w_{1,x}) - kG(H-h)(\psi_2 + w_{2,x}) - kGh(\psi_3 + w_{3,x})] + (P_3 w_{3,x} + P_2 w_{2,x} - P_1 w_{1,x}) = 0 \quad \text{at} \quad x = a \tag{20}$$

which are the moment balance condition and shear force balance condition at the delamination front, respectively. With a Griffith-type fracture criterion, the local growth condition at the delamination front for a quasistatic process is

$$\Gamma^* = \Gamma \tag{21}$$

Γ is the energy release rate at the delamination front given by

$$\Gamma = \frac{1 - \nu_{13}\nu_{31}}{2E}\left(\frac{P_2^2}{H-h} + \frac{P_3^2}{h} - \frac{P_1^2}{H}\right) + \frac{1}{2}\left(\frac{M_2^2}{D_2} + \frac{M_3^2}{D_3} - \frac{M_1^2}{D_1}\right) + \frac{1}{2}\left(\frac{Q_1^2}{kGH} - \frac{Q_2^2}{kG(H-h)} - \frac{Q_3^2}{kGh}\right) + \frac{1}{2}(P_2 w_{2,x}^2 + P_3 w_{3,x}^2 - P_1 w_{1,x}^2) \quad \text{at} \quad x = a \tag{22}$$

where

$$M_i = D_i\psi_{i,x}, \qquad Q_i = kGh_i(\psi_i + w_{i,x}) \qquad i = 1,2,3 \tag{23}$$

are the bending moments and transverse shear forces of the corresponding sublaminate. In Eq. (22), the energy release rate is expressed analytically in terms of the axial forces, bending moments, transverse shear forces, and slopes of the deflections of the three sublaminates at the delamination front in the postbuckling configuration. In the expression of energy release rate given by Kardomateas and Schmueser,[16] although the transverse shear effect through membrane forces and bending moments (terms inside the first two parentheses) is considered, the effect on the energy release rate due to the terms inside the last two parentheses in Eq. (21) is not included. However, the formulation based on the energy principle shows that these terms will appear and should not be omitted if the transverse shear is included.

Delamination Buckling and Postbuckling States

From the equations of equilibrium [Eqs. (15) and (16)], the deflections and rotations of the three sublaminates can be expressed as

$$w_1 = A\{1 - \cos\lambda_1(l-x)\}, \qquad a \le x \le l \tag{24a}$$

$$w_2 = A\left\{\frac{(1-s\bar{P}_1)}{(1-s\bar{P}_2)/(1-\bar{h})}\frac{\lambda_1 \sin\lambda_1 b}{\lambda_2 \sin\lambda_2 a}(\cos\lambda_2 x - \cos\lambda_2 a) + 1 - \cos\lambda_1 b\right\}, \qquad 0 \le x \le a \tag{24b}$$

$$w_3 = A\left\{\frac{(1-s\bar{P}_1)}{(1-s\bar{P}_3)/\bar{h}}\frac{\lambda_1 \sin\lambda_1 b}{\lambda_3 \sin\lambda_3 a}(\cos\lambda_3 x - \cos\lambda_3 a) + 1 - \cos\lambda_1 b\right\}, \qquad 0 \le x \le a \tag{24c}$$

$$\psi_1 = (1-s\bar{P}_1)A\lambda_1 \sin\lambda_1(l-x), \qquad a \le x \le l \tag{25a}$$

$$\psi_2 = (1-s\bar{P}_1)A\frac{\lambda_1 \sin\lambda_1 b}{\sin\lambda_2 a}\sin\lambda_2 x, \qquad 0 \le x \le a \tag{25b}$$

$$\psi_3 = (1-s\bar{P}_1)A\frac{\lambda_1 \sin\lambda_1 b}{\sin\lambda_3 a}\sin\lambda_3 x, \qquad 0 \le x \le a \tag{25c}$$

where

$$b = l - a, \qquad \bar{h} = \frac{h}{H}, \qquad \bar{P}_i = \frac{P_i}{(\pi^2 D_1/l^2)}, \qquad i = 1,2,3$$

$$s = \frac{\pi^2 D_1}{kGHl^2} = \frac{\pi^2}{12(1-\nu_{13}\nu_{31})}\frac{E}{kG}\left(\frac{H}{l}\right)^2$$

$$\lambda_1^2 = \frac{1}{1-s\bar{P}_1}\frac{P_1}{D_1}, \qquad \lambda_2^2 = \frac{1}{1-[(s\bar{P}_2/(1-\bar{h})]}\frac{P_2}{D_2}, \qquad \lambda_3^2 = \frac{1}{1-[(s\bar{P}_3/\bar{h})]}\frac{P_3}{D_3} \tag{26}$$

It is noted that Eqs. (24) and (25) satisfy Eqs. (1-4), (18), and (20). In these expressions, the terms with parameter s are due to the transverse shear effect. For loading controlled problems, the compressive load P_1 is given, whereas the amplitude A, and the compressive loads P_2 and P_3 of both lower and upper sublaminates are determined from axial force balance condition [Eq. (5)], compatibility condition of axial displacement [Eq. (6)], and moment balance condition at the delamination front [Eq. (19)]. Substituting Eqs. (24) and (25) into Eqs. (5), (6), and (19), we get

$$\left(\frac{A\lambda_1 \sin\lambda_1 b}{2}\right)^2\left\{\left[\frac{1-s\bar{P}_1}{1-(s\bar{P}_3/\bar{h})}\right]^2\left(\frac{1}{\sin^2\lambda_3 a} - \frac{1}{\lambda_3 a \tan\lambda_3 a}\right) - \left\{\frac{1-s\bar{P}_1}{1-[(s\bar{P}_2/(1-\bar{h})]}\right\}^2\left(\frac{1}{\sin^2\lambda_2 a} - \frac{1}{\lambda_2 a \tan\lambda_2 a}\right)\right\} + (1-s\bar{P}_1)\frac{H}{a}\left(\frac{A\lambda_1 \sin\lambda_1 b}{2}\right) + \frac{1-\nu_{13}\nu_{31}}{E}\left(\frac{P_3}{h} - \frac{P_1 - P_3}{H-h}\right) = 0 \tag{27}$$

$$\left(\frac{A\lambda_1 \sin\lambda_1 b}{2}\right)(1-s\bar{P}_1)\{\bar{h}^3\lambda_3 \cot\lambda_3 a + (1-\bar{h})^3\lambda_2 \cot\lambda_2 a + \lambda_1 \cot\lambda_1 b\} - \frac{3(1-\nu_{13}\nu_{31})}{EH^3}(HP_3 - hP_1) = 0 \tag{28}$$

With Eqs. (5) and (26), Eqs. (27) and (28) provide two nonlinear algebraic equations for two unknowns, P_3 and A. The deflections w_i and rotations ψ_i in the three sublaminates of the postbuckling solution are then obtained from Eqs. (24) and (25). For displacement-controlled problems, the axial shortening Δ is given and Eqs. (27) and (28) involve three unknowns, P_1, P_3, and A, so that one more equation is needed that can be provided by the kinematic relation of axial shortening [Eq. (7)] to obtain these three unknowns.

Following arguments similar to that in Yin et al.,[9] the characteristic equation of delamination buckling load can be written as

$$\text{ctn}\,(\lambda_1 b) + (1-\bar{h})^2 \text{ctn}\left(\frac{\lambda_1 a}{1-\bar{h}}\right) + \bar{h}^2 \text{ctn}\left(\frac{\lambda_1 a}{\bar{h}}\right) + \frac{3\bar{h}(1-\bar{h})}{\lambda_1 a} = 0 \tag{29}$$

The critical value of λ_1 calculated from Eq. (29) is identical to that in Yin et al.[9] However, because this loading parameter λ_1 is defined differently, the corresponding critical buckling load P_1 is different with the shear effect included. From the definition of λ_1 given by Eq. (26), the relation between critical buckling loads with ($s \neq 0$) and without ($s = 0$) transverse shear effect can be expressed as

$$(\bar{P}_{1\text{cr}})_s = \frac{(\bar{P}_{1\text{cr}})_c}{1 + s(\bar{P}_{1\text{cr}})_c} \tag{30}$$

where the subscripts s and c denote shear deformation theory and classical lamination theory, respectively. It is seen from Eq. (30) that the effect of shear deformation will reduce the delamination critical buckling load. The normalized delamination buckling loads $\bar{P}_1$ for different length ratio $\bar{a} = a/l$ and thickness ratio $\bar{h} = h/H$ are calculated and the results are compared with those without the transverse shear effect[8] and shown in Table 1. The shear deformation parameter s defined by Eq. (25) represents the extent of transverse shear effect and is set to be 0.2 in Table 1. The delamination buckling load varies with the parameter s, the length ratio $\bar{a}$, and the thickness ratio $\bar{h}$. If the material of the delaminated plate is fixed, then the transverse shear effect depends on the relative slenderness ratio $\bar{a}/\bar{h}$. From Table 1, it can be seen that the difference between the buckling loads calculated with and without the transverse shear effect decreases as the relative slenderness ratio increases. The difference is less than 1% if the relative slenderness ratio is greater than 5. Roughly speaking, if the value of $\bar{a}/\bar{h}$ is less than 1, the transverse shear effect becomes significant and should not be neglected.

If the shear deformation parameter s is set to be zero, i.e., the transverse shear effect is not included, then all of the governing equations can be reduced to the same as those in Yin et al.[9] and the critical buckling load and the corresponding postbuckling solution are the same as those derived from the classical lamination theory. For the composite materials of graphite/epoxy, boron/epoxy, and aramid/epoxy,[17] with the ratio of length to thickness $2l/H$ around 10–50, the shear deformation parameter s will be in the range of 0.04–1.5.

Without loss of generality, the thickness ratio of upper sublaminate $\bar{h}$ is assumed to be in the range of 0–0.5. Depending on the value of the relative slenderness ratio $\bar{a}/\bar{h}$, two extreme buckling configurations can be observed. These two extreme configurations, named as near global and near local buckling modes, respectively, occur when the relative slenderness ratios are extremely small or extremely large, say, < 0.1 and > 10, respectively. Figures 2 show these two extreme configurations. However, for the intermediate value of $\bar{a}/\bar{h}$ between these two extremes, general postbuckling behavior of delaminated plate is observed and distinguishable deflections of upper and lower sublaminates are noticed. Two distinctive postbuckling behaviors can be observed for the general buckling configuration (see Figs. 3). For cases of short and thick delaminations (i.e., small relative slenderness ratio), both upper and lower sublaminates deflect upward (see Fig. 3a) and the contact of these two sublaminates will take place in the postbuckling states. Figure 4 illustrates the normalized midpoint deflections of both lower and upper sublaminates $\bar{w}_2$ and $\bar{w}_3$, which are defined as w_2/H and w_3/H, respectively, from the buckling state to the state of contact for three different values of shear deformation parameters. The results indicate that the contact of upper and lower sublaminates occurs almost immediately after the ultimate load is attained for small shear deformation parameters. If the shear deformation parameter becomes larger, then the state of contact may be

Table 1 Delamination buckling loads $\bar{P}_1$

		h/H						
a/L		0.02	0.05	0.10	0.20	0.30	0.40	0.50
0.025	SDT[a]	0.56738	0.83333	0.83333	0.83333	0.83333	0.83333	0.83333
	CLT[b]	0.64000	1.00000	1.00000	1.00000	1.00000	1.00000	1.00000
0.05	SDT	0.15504	0.82981	0.83332	0.83333	0.83333	0.83333	0.83333
	CLT	0.16000	0.99493	0.99998	0.99999	0.99999	1.00000	1.00000
0.10	SDT	0.03968	0.23804	0.81934	0.83313	0.83322	0.83324	0.83324
	CLT	0.04000	0.24994	0.97992	0.99971	0.99983	0.99986	0.99987
0.15	SDT	0.01772	0.10868	0.40733	0.83095	0.83231	0.83256	0.83262
	CLT	0.01778	0.11109	0.44346	0.99657	0.99852	0.99889	0.99898
0.20	SDT	0.00998	0.06173	0.23767	0.78162	0.82804	0.82989	0.83025
	CLT	0.01000	0.06250	0.24953	0.92644	0.99239	0.99504	0.99556
0.25	SDT	0.00639	0.03968	0.15479	0.55601	0.80972	0.82186	0.82354
	CLT	0.00640	0.04000	0.15973	0.62557	0.96619	0.98353	0.98593
0.30	SDT	0.00444	0.02762	0.10853	0.40197	0.73249	0.80137	0.80806
	CLT	0.00444	0.02777	0.11094	0.43711	0.85822	0.95433	0.96383
0.40	SDT	0.00250	0.01557	0.06165	0.23542	0.48033	0.68094	0.73092
	CLT	0.00250	0.01562	0.06242	0.24705	0.53138	0.78830	0.85606
0.50	SDT	0.00160	0.00998	0.03968	0.15368	0.32439	0.50969	0.60599
	CLT	0.00160	0.01000	0.04000	0.15855	0.34690	0.56754	0.68956
0.60	SDT	0.00111	0.00693	0.02761	0.10796	0.23222	0.38097	0.48829
	CLT	0.00111	0.00694	0.02776	0.11034	0.24353	0.41239	0.54114
0.70	SDT	0.00082	0.00509	0.02032	0.07992	0.17408	0.29288	0.39677
	CLT	0.00082	0.00510	0.02040	0.08122	0.18036	0.31110	0.43097
0.80	SDT	0.00063	0.00391	0.01557	0.06152	0.13525	0.23156	0.32834
	CLT	0.00063	0.00391	0.01562	0.06229	0.13901	0.24281	0.35142
0.90	SDT	0.00049	0.00309	0.01231	0.04882	0.10811	0.18756	0.27705
	CLT	0.00049	0.00309	0.01234	0.04930	0.11050	0.19487	0.29330

[a]SDT = shear deformation theory ($s = 0.2$). [b]CLT = classical lamination theory.

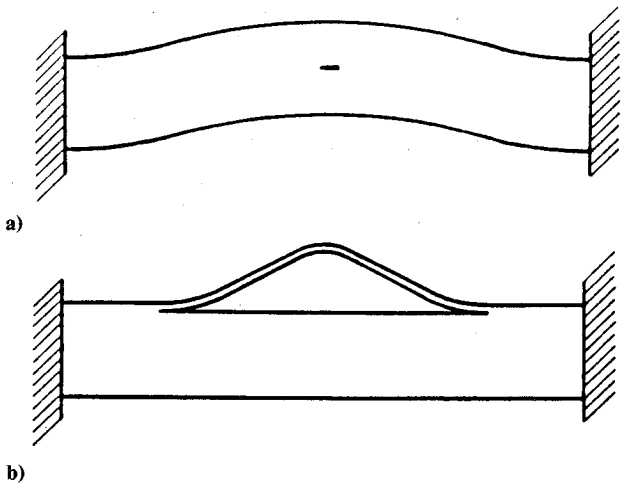

Fig. 2 Extreme buckling configurations: a) near global buckling; b) near local buckling.

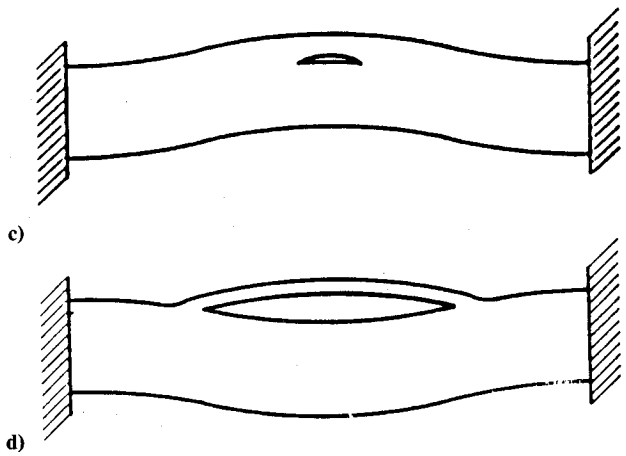

Fig. 3 General buckling configurations: a) short and thick delamination; b) long and thin delamination.

attained before the ultimate load is reached. Since the critical buckling load does not deviate too much from the ultimate load, it can be used as a closed lower bound of the ultimate compressive load capacity of the delaminated laminate. For cases of long and thin delaminations (i.e., large relative slenderness ratio), as discussed by Yin et al.,[9] a transition postbuckling solution exists in the present analysis. The transition solution is a special postbuckling solution that cannot be obtained from the general solution of the problem and occurs only for a plate with long delamination under appropriate axial load. For plates with long and thin delaminations, there exist two different phases of solution—the initial postbuckling phase and the secondary postbuckling phase; the transition postbuckling solution is the boundary between them. In the initial postbuckling phase, both upper and lower sublaminates deflect upward. However, beyond the transition state, the secondary postbuckling phase takes place and the upper and lower sublaminates begin to deflect in opposite directions, i.e., the lower sublaminate turns to deflect downward (see Fig. 3b). From a mathematical point of view, the transition postbuckling state occurs when the denominators in Eqs. (24c) and (25c) vanish, i.e., $\lambda_3 a = \pi$. The postbuckling solution corresponding to this state can be expressed in the following form:

$$w_1(x) = w_2(x) = 0 \tag{31a}$$

$$w_3(x) = B\left(1 + \cos\frac{\pi x}{a}\right) \tag{31b}$$

$$\psi_1(x) = \psi_2(x) = 0 \tag{31c}$$

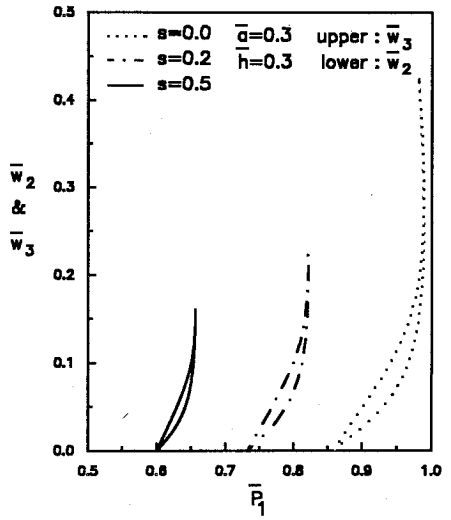

Fig. 4 Midpoint deflections of upper and lower sublaminates.

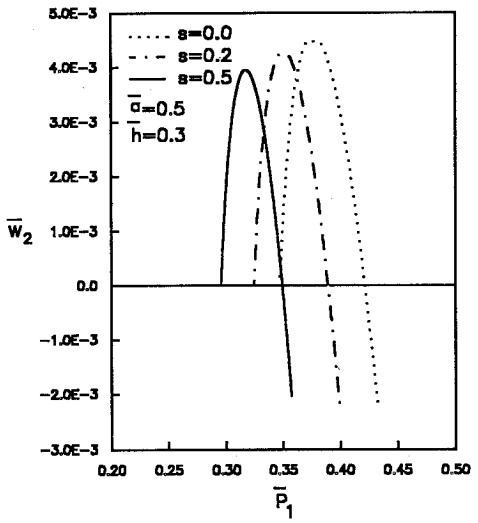

Fig. 5 Midpoint deflection of lower sublaminates.

$$\psi_3(x) = B\left(1 + \frac{s\bar{h}^2}{\bar{a}^2}\right)^{-1} \frac{\pi}{a} \sin\frac{\pi x}{a} \tag{31d}$$

With Eqs. (5), (6), and (19), the amplitude B and the axial compressive load P_1 corresponding to the transition state can be determined as

$$B = \frac{2h^2}{3(1-h)}\left(1 + \frac{s\bar{h}^2}{\bar{a}^2}\right)^{-1}$$

$$P_1 = D_1\left(\frac{\pi\bar{h}}{a}\right)^2\left[1 + \left(1 + \frac{s\bar{h}^2}{\bar{a}^2}\right)^{-1}\frac{4\bar{h}^2}{3(1-\bar{h})}\right]\left(1 + \frac{s\bar{h}^2}{\bar{a}^2}\right)^{-1} \tag{32}$$

From the present analysis, it is observed that the transition state occurs at lower axial load if the transverse shear effect is considered. Figure 5 shows the normalized midpoint deflection $\bar{w}_2$ of the lower sublaminate under axial load close to the delamination buckling load with three different shear deformation parameters. The transition states are clearly seen in the figure and it is found that the maximum upward deflection decreases as the shear deformation parameter increases. Figure 6 illustrates the normalized midpoint deflections of both upper and lower sublaminates for a wide range of axial load. From the calculated results, it is observed that the axial compressive load can be significantly greater than the critical buckling load. Since the energy release rate Γ may be greater

than the specific fracture energy Γ^* of the material during the postbuckling stage, the ultimate compressive load capacity is governed by the postbuckling solution and the progressive delamination growth. It is indicated that the effect of transverse shear is to lower the ultimate load capacity with the reduced extent depending on the ratio of inplane axial Young's modulus and transverse shear modulus E/G, the length ratio $\bar{a}$, and thickness ratio $\bar{h}$.

Energy Release Rate and Delamination Growth

After the initiation of delamination buckling, the occurrence of the delamination growth depends on the magnitude of the fracture toughness of the material Γ^*. The energy release rate Γ evaluated by Eq. (22) from the postbuckling solution is required to predict the delamination growth. During the postbuckling stage, only when the local delamination growth condition Eq. (21) is satisfied, the progression of delamination arises.

The transverse shear effect on the energy release rate is illustrated in Figs. 7–9. The variations of the normalized axial load $\bar{P}_1$ with the nondimensionalized energy release rate, $\bar{\Gamma}=\Gamma/(D_1H^2/l^4)$, for three sets of length ratio $\bar{a}$ and thickness ratio $\bar{h}$ and various values of shear deformation parameter s are shown in these figures. It is observed that with the same applied load, the energy release rate $\bar{\Gamma}$ increases as the shear deformation parameter s increases. Therefore, the initiation of delamination growth will occur at lower applied load than that predicted by the classical lamination theory. Note that a logarithmic scale is used to represent $\bar{\Gamma}$, which indicates that the transverse shear effect is significant and should not be neglected. The relative slenderness ratios $\bar{a}/\bar{h}$ in Figs. 7–9 are 1, 1.67, and 9, respectively. For the case of small relative slenderness ratio $\bar{a}/\bar{h}=1$ (Fig. 7), each curve ends with the state of contact. The difference between curves with different values of parameter s is manifest. The initial buckling loads and ultimate loads are quite different for various values of parameter s. For the case of medium relative slenderness ratio $\bar{a}/\bar{h}=1.67$ (Fig. 8), the difference between various curves are not so large for $\bar{\Gamma}<10^{-1}$ compared with Fig. 7. For the case of large relative slenderness ratio $\bar{a}/\bar{h}=9$ (Fig. 9), the variations of $\bar{P}_1$ with $\bar{\Gamma}$ are negligibly small for values of $\bar{P}_1<0.3$ and the initial buckling loads are almost identical for different parameter s. However, significant differences between curves are seen at larger values of $\bar{P}_1$ in Figs. 8 and 9. Figure 10 illustrates the variations of $\bar{P}_1$ with $\bar{\Gamma}$ for various values of $\bar{a}$ with $\bar{h}=0.3$ and $s=0.2$. Since in a quasistatic process of delamination growth, the energy release rate $\bar{\Gamma}$ remains constant and is equal to the critical value $\bar{\Gamma}^*=\Gamma^*/(D_1H^2/l^4)$, once $\bar{\Gamma}^*$ is given, the initiation of the delamination growth and the behavior thereafter (i.e., stable or catastrophic growth) can be determined from Fig. 10. It is observed from Fig. 10 that, except for the entangled region with the values of $\bar{\Gamma}^*$ around 0.1–0.4 and $\bar{a}$

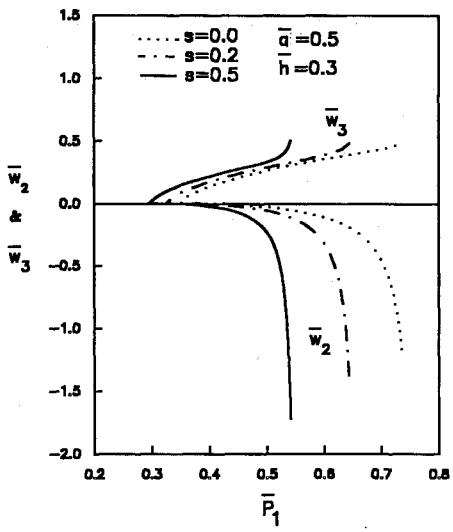

Fig. 6 Midpoint deflections of upper and lower sublaminates.

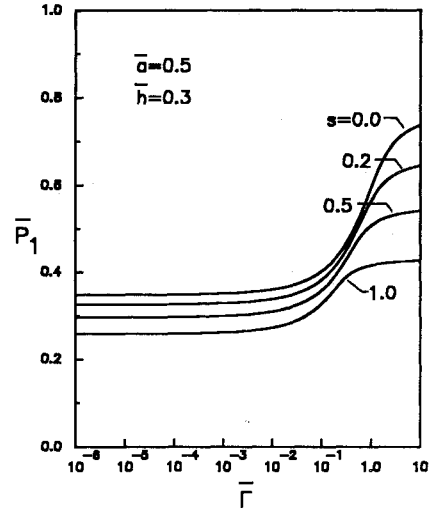

Fig. 8 Variation of energy release rate with axial load, $\bar{a}=0.5$ and $\bar{h}=0.3$.

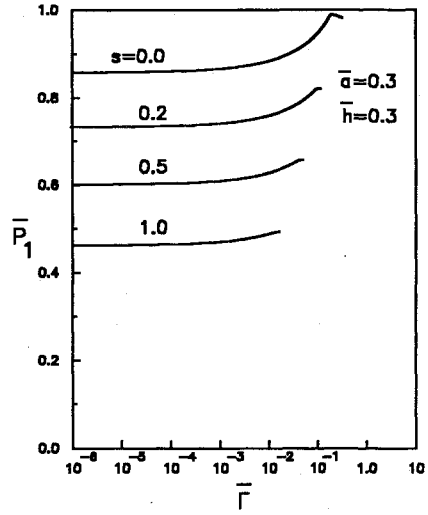

Fig. 7 Variation of energy release rate with axial load, $\bar{a}=0.3$ and $\bar{h}=0.3$.

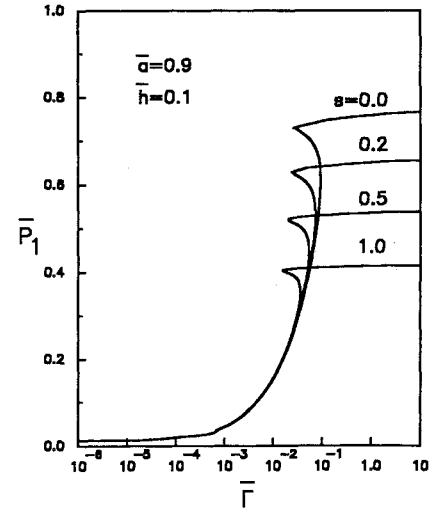

Fig. 9 Variation of energy release rate with axial load, $\bar{a}=0.9$ and $\bar{h}=0.1$.

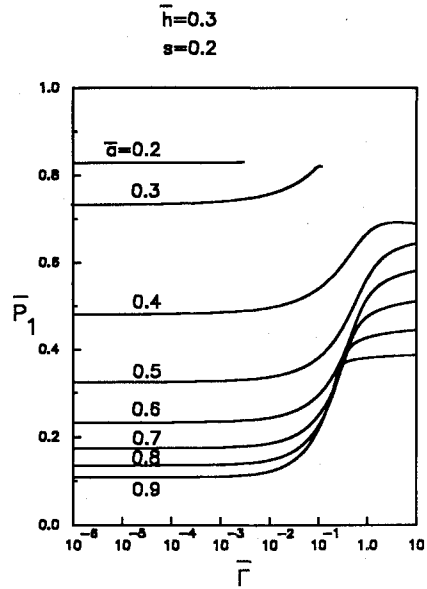

Fig. 10 Variation of energy release rate with axial load, $\bar{h}=0.3$ and $\bar{s}=0.2$.

around 0.6–0.9, the catastrophic process prevails under constant axial load $\bar{P}_1$ once the delamination growth occurs. For the loading controlled problem, the complete behavior of delamination growth can be determined for fixed values of $\bar{h}$ and s if variations of $\bar{P}_1$ with $\bar{\Gamma}$ are plotted for this set of values of $\bar{h}$ and s. Similar plots can be used to determine the behavior of delamination growth for displacement control condition.

Conclusions

A variational-principle-consistent shear deformation theory is used to formulate the delamination buckling and growth problem. The delamination buckling load is determined by a nonlinear characteristic equation and the postbuckling solution is governed by two nonlinear algebraic equations for the load control case and three nonlinear algebraic equations for the displacement control case. Analytic form of strain energy release rate is derived from the variational principle. It is shown that the transverse shear effect on buckling load, postbuckling solution, and energy release rate is significant.

Acknowledgment

This research work was supported by the National Science Foundation Grant ECS-9003883 and the scholarly and creative activity summer fellowship provided by the California State University, Long Beach.

References

[1]Chai, H., Babcock, C. D., and Knauss, W. G., "One Dimensional Modeling of Failure in Laminated Plates by Delamination Buckling," *International Journal of Solids and Structures*, Vol. 17, No. 11, 1981, pp. 1069–1083.

[2]Whitcomb, J. D., "Finite Element Analysis of Instability Related Delamination Growth," *Journal of Composite Materials*, Vol. 15, Sept. 1981, pp. 403–426.

[3]Chai, H., and Babcock, C. D., "Two-Dimensional Modelling of Compressive Failure in Delaminated Laminates," *Journal of Composite Materials*, Vol. 19, Jan. 1985, pp. 67–95.

[4]Yin, W. L., "Axisymmetric Buckling and Growth of a Circular Delamination in a Compressed Laminate," *International Journal of Solids and Structures*, Vol. 21, No. 5, 1985, pp. 503–514.

[5]Bottega, W. J., and Maewal, A., "Delamination Buckling and Growth in Laminates," *Journal of Applied Mechanics*, Vol. 50, March 1983, pp. 184–189.

[6]Shivakumar, K. N., and Whitcomb, J. D., "Buckling of a Sublaminate in a Quasi-Isotropic Composite Laminate," NASA TM-85755, 1984.

[7]Whitcomb, J. D., "Parametric Analytical Study of Instability Related Delamination Growth," *Composites Science and Technology*, Vol. 25, 1986, pp. 19–48.

[8]Simitses, G. J., Sallam, S. N., and Yin, W. L., "Effect of Delamination of Axially Loaded Homogeneous Laminated Plates," *AIAA Journal*, Vol. 23, No. 9, 1985, pp. 1437–1445.

[9]Yin, W. L., Sallam, S. N., and Simitses, G. J., "Ultimate Axial Load Capacity of a Delaminated Beam-Plate," *AIAA Journal*, Vol. 24, No. 1, 1986, pp. 123–128.

[10]Yin, W. L., and Jane, K., "Postbuckling Analysis of Laminated Elliptical Plates with Application to Delamination Growth," *Proceedings of the AIAA/ASME/ASCE/AHS/ASC 30th Structures, Structural Dynamics and Materials Conference*, AIAA, Washington, DC, 1989, pp. 121–134.

[11]Chow, C. L., and Ngan, K. M., "Method of Fracture Toughness Evaluation of Adhesive Joints," *Journal of Strain Analysis*, Vol. 15, 1980, pp. 97–101.

[12]Yin, W. L., and Wang, J. T. S., "The Energy Release Rate in the Growth of a One-Dimensional Delamination," *Journal of Applied Mechanics*, Vol. 51, 1984, pp. 939–941.

[13]Yin, W. L., "Energy Balance and the Speed of Crack Growth in a Buckled Strip Delamination," *Proceedings of the AIAA/ASME/ASCE/AHS/ASC 28th Structures, Structural Dynamics, and Materials Conference*, AIAA, New York, 1987, pp. 748–765.

[14]Chen, H. P., and Yin, W. L., " Dynamic Analysis of Delamination Growth in a Compressed Laminate," *Computational Mechanics '88 Theory and Applications*, Vol. 1, edited by S. N. Atluri and G. Yagawa, Springer-Verlag, Berlin, 1988.

[15]Chen, H. P., and Ngo, H., "Dynamic Analysis of Delamination Growth," *Proceedings of the AIAA/ASME/ASCE/AHS/ASC 30th Structures, Structural Dynamics, and Materials Conference*, AIAA, Washington, DC, 1989, pp. 1264–1272.

[16]Kardomateas, G. A., and Schmueser, D. W., "Effect of Transverse Shearing Forces on Buckling and Postbuckling of Delaminated Composites under Compressive Loads," *Proceedings of the AIAA/ASME/ASCE/AHS/ASC 28th Structures, Structural Dynamics and Materials Conference*, AIAA, New York, 1987, pp. 757–765.

[17]Tsai, S. W., and Hahn, H. T., *Introduction to Composite Materials*, Technomic, Lancaster, PA, 1980.